Rate and Equilibrium Study of the Reversible Oxidative Addition of Silanes to the Iridium Center in $Cp_2Ta(\mu\text{-}CH_2)_2Ir(CO)_2$ and of Alkene Hydrosilation/ Isomerization Catalyzed by This System

Michael J. Hostetler, Matthew D. Butts, and Robert G. Bergman*

Department of Chemistry, University of California, Berkeley, California 94720

Received March 18, 1992

The mechanism of the catalytic hydrosilation of ethylene by the early–late transition metal heterodinuclear complex $Cp_2Ta(\mu\text{-}CH_2)_2Ir(CO)_2$ (1) has been studied. The second-order rate constant for catalytic ethylene hydrosilation at 45 °C in toluene-d_8 is $(2.65 \pm 0.43) \times 10^{-3}$ M^{-1} s^{-1}; the rate is dependent upon [1] and [C_2H_4] but is independent of [Et_3SiH]. We have found that the first step in the catalytic reaction is the oxidative addition of R_3SiH to form $Cp_2Ta(\mu\text{-}CH_2)_2Ir(SiR_3)(H)(CO)_2$ [R = Me (**2a**); Et (**2b**); Ph (**2c**)], which is in equilibrium with 1 and free silane. In all three cases, only the cis Si/H isomer, in which the hydride is trans to a CO and the silane trans to a μ-CH_2, is detectable over a range of temperatures. The thermodynamic parameters for all three reactions have been measured in THF-d_8: **2a**, $\Delta H°$ (−9.60 ± 0.45 kcal/mol), $\Delta S°$ (−19.1 ± 1.5 eu); **2b**, $\Delta H°$ (−10.8 ± 0.4 kcal/mol), $\Delta S°$ (−24.8 ± 1.4 eu); **2c**, $\Delta H°$ (−12.4 ± 0.4 kcal/mol), $\Delta S°$ (−24.0 ± 1.4 eu). The parameters were also measured for **2b** in toluene-d_8: $\Delta H°$ (−11.2 ± 0.7 kcal/mol), $\Delta S°$ (−25.0 ± 2.5 eu). The rate of oxidative addition of Et_3SiH to 1 was found to be first-order in [Et_3SiH] and [1]; at 0 °C in toluene the second-order rate constant is 3.57 ± 0.07 M^{-1} s^{-1} and in THF, 2.16 ± 0.03 M^{-1} s^{-1}. The primary kinetic isotope effect for this reaction was measured to be 1.13. The reductive elimination of Et_3SiH from **2b** at 0 °C in toluene has a rate constant of $(1.20 \pm 0.02) \times 10^{-3}$ s^{-1} in toluene and $(1.32 \pm 0.02) \times 10^{-3}$ s^{-1} in THF. The primary kinetic isotope effect for this step was calculated to be 1.45. The activation parameters for the addition of Et_3SiH have also been measured: $\Delta H^‡ = 9.4 \pm 0.2$ kcal/mol and $\Delta S^‡ = -21.1$ eu, and for the reductive elimination of Et_3SiH from **2b**: $\Delta H^‡ = 20.6 \pm 0.2$ kcal/mol and $\Delta S^‡ = 3.9$ eu. The reaction of Et_3SiD with 1 results in the incorporation of deuterium into the methylene bridges. We suggest that this reaction occurs by oxidative addition of Et_3SiD, reductive elimination of a μ-methylene deuteride to form a $TaCH_2D$ group, C–H oxidative addition of this group across the iridium center, and reductive elimination of Et_3SiH. We have studied the kinetics of this reaction and found that the rate is dependent upon [1] and independent of [Et_3SiD] (since addition of more than 2 equiv of Et_3SiD drives the equilibrium completely toward **2b**) and that the rate constant at 10 °C is $(6.46 \pm 0.82) \times 10^{-4}$ s^{-1}. The activation parameters for this process have been measured: $\Delta H^‡ = 15.8 \pm 1.2$ kcal/mol and $\Delta S^‡ = -17 \pm 5$ eu. However, this reaction pathway for deuterium exchange is not thought to be along the route for catalytic hydrosilation because addition of CO to the reaction mixture severely inhibits the reaction. Instead, after oxidative addition of R_3SiH, a CO ligand dissociates to create an open coordination site. Ethylene then binds to the iridium center, inserts into the Ir–H bond (at this point β-elimination can occur, and in the case of substituted alkenes results in isomerization without hydrosilation), and reductive elimination of an ethyl and a silyl group completes the catalytic cycle.

The hydrosilation of alkenes is an important industrial[1] and laboratory process in which an Si–H bond adds across a carbon–carbon double bond. Chalk and Harrod offered the first detailed set of studies concerning the mechanism for this reaction: R_3SiH first oxidatively adds to the M(alkene) complex, followed by alkene insertion into the M–H bond and reductive elimination of the alkyl and silyl groups to form the new silane (Scheme I, mechanism A).[2-4] In order to explain the formation of vinylsilanes, a modification of this mechanism was proposed, in which alkene also inserts into the M–Si bond (Scheme I, mechanism B).[5] Recently, a new type of hydrosilation mechanism has been proposed to explain the catalytic behavior of $CpRh(C_2H_4)(SiR_3)H$ (Scheme II).[6,7]

However, these mechanisms were not able to explain why some catalysts needed oxygen or a variable initiation period in order to be active. This led Lewis to propose that certain active hydrosilation catalysts are colloids, formed from interaction of the metal complex with oxygen and silane.[8-10]

(1) Noll, W. *Chemistry and Technology of Silicones*; Academic Press: New York, 1968.
(2) Ojima, I. In *The Chemistry of Organic Silicon Compounds*; Patai, S., Rappoport, Z., Eds.; John Wiley & Sons, Ltd.: New York, 1989; p 1479.
(3) Speier, J. L. *Adv. Organomet. Chem.* **1979**, *17*, 407.
(4) Harrod, J. F.; Chalk, A. J. In *Organic Synthesis with Metal Carbonyls*; Wender, I., Pino, P. Eds.; Wiley: New York, 1977; Vol. 2, p 673.
(5) Tilley, T. D. In *The Chemistry of Organic Silicon Compounds*; Patai, S., Rappoport, Z., Eds.; John Wiley & Sons Ltd: New York, 1989; p 1415.
(6) Duckett, S. B.; Perutz, R. N. *Organometallics* **1992**, *11*, 90.
(7) Scheme II is a modification of the mechanism proposed for the hydrosilation of alkenes catalyzed by $Co(CO)_4SiR_3$. Seitz, F.; Wrighton, M. S. *Angew. Chem., Int. Ed. Engl.* **1988**, *27*, 289.

0276-7333/93/2312-0065$04.00/0

Scheme I

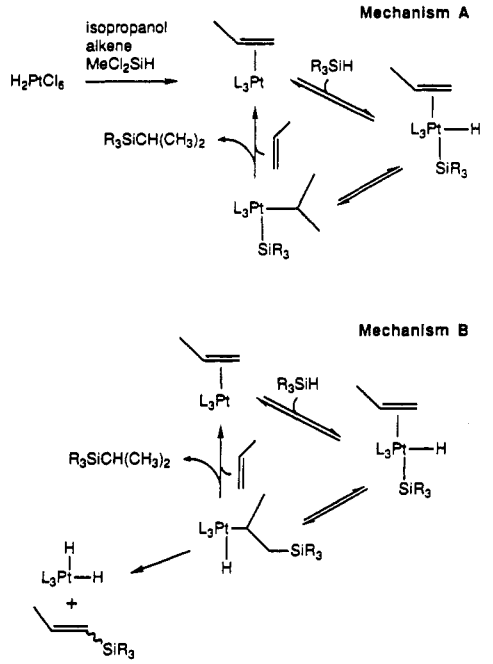

Scheme II

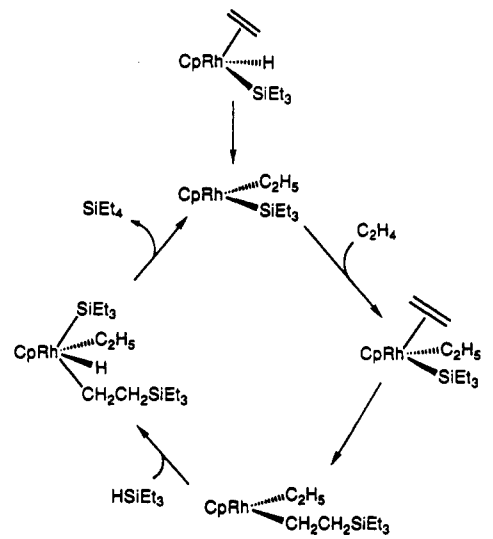

Recently, we reported[11] that the complex $Cp_2Ta(\mu\text{-}CH_2)_2Ir(CO)_2$ (1) catalytically hydrosilates ethylene. Compound 1 does not require O_2 or an initiation period in order to be active, and (on the basis of its continued reactivity in the presence of Hg) it appears to be a homogeneous catalyst. This paper reports a study of some of the steps involved in the overall reaction mechanism.

Results

Hydrosilation Reactions. Compound 1 is a catalyst precursor for the hydrosilation of ethylene at 45 °C (Scheme III). The metal species exclusively detectable in solution during catalysis is the silane oxidative addition product **2b**. Unlike some hydrosilation catalysts, compound 1 does not require either addition of oxygen or an initiation period in order to be active. Addition of 100 equiv of mercury to a hydrosilation solution does not result in catalyst decomposition or loss of activity. Conversely, addition of CO severely inhibits the rate.

Scheme III

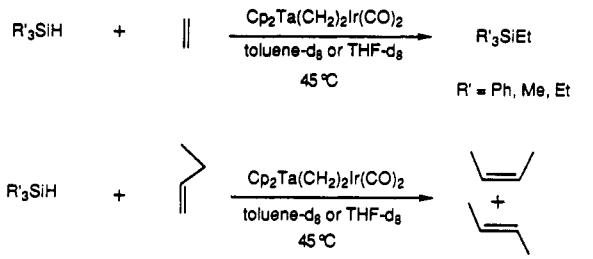

Most of our studies were performed with Et_3SiH, although Me_3SiH and Ph_3SiH can be used as well. Use of disubstituted silanes or silanes containing alkoxide or halide substituents resulted only in catalyst decomposition. Higher alkenes such as 1-butene are not hydrosilated but are isomerized to a mixture of *cis*- and *trans*-2-butene (Scheme III); isomerization does not occur in the absence of R_3SiH. The isomerization reaction proceeds about 2–3 times more slowly than the hydrosilation of ethylene. Use of Et_3SiD in the hydrosilation of ethylene resulted in the incorporation of D into the $TaCH_2Ir$ positions much more rapidly than formation of Et_4Si (see below).

The predominant product of the ethylene hydrosilation reaction is tetraethylsilane. This contrasts with the results of certain other studies, in which substantial amounts of vinylsilanes are produced.[6,12] For example, in the Maitlis study[12] a 7/1 ratio of hex-1-ene to Et_3SiH led to approximately 85% vinylsilanes, and in the Perutz work[6] an 80% vinylsilane yield was reached at only a 4:3 ratio of ethylene to triethylsilane. Because of the highly coupled nature of the vinyl protons in triethylvinylsilane, and the fact that we monitored our reactions mainly by NMR spectrometry, we at first believed that little or no triethylvinylsilane was formed in this system. However, at the suggestion of a thoughtful reviewer we used both NMR and gas chromatography to search carefully for this unsaturated product. While the amounts observed are somewhat erratic (for reasons we do not understand) it is now clear that 10–30% yields of vinylsilane are reproducibly formed. The variation in vinylsilane yield does not appear to be an analytical problem: monitoring hydrosilation reactions by NMR indicated that the yield of vinylsilane is not dependent upon the extent of conversion and established that the vinylsilane was stable to the reaction conditions; yields of vinylsilane measured by NMR and gas chromatography were in good agreement. Addition of CO did not seem to affect the amounts of vinylsilane formed. In contrast to the behavior of the systems described earlier, we do not see a dramatic increase in vinylsilane yield with increasing olefin/silane ratio. Over a reasonable range of catalyst/ethylene/silane ratios, the vinylsilane/triethylsilane ratios vary almost randomly between 10 and 30%, and no clear dependence on concentration is observed (see Table X and the Experimental Section).

Determination of the Rate Law for Hydrosilation. The rate of ethylene hydrosilation catalyzed by 1 was studied in toluene-d_8 at 45 °C (Figure 1; Table I). In our preliminary communication[11] we reported that the rate was first-order in the concentration of silane and zero-

(8) Hostetler, M. J.; Bergman, R. G. *J. Am. Chem. Soc.* **1990**, *112*, 8621.
(9) Lewis, L. N.; Lewis, N. *Chem. Mater.* **1989**, *1*, 106.
(10) Lewis, L. N. *J. Am. Chem. Soc.* **1990**, *112*, 5998.
(11) Lewis, L. N.; Uriarte, R. J. *Organometallics* **1990**, *9*, 621.
(12) Millan, A.; Fernandez, M.-J.; Bentz, P.; Maitlis, P. M. *J. Mol. Catal.* **1984**, *26*, 89.

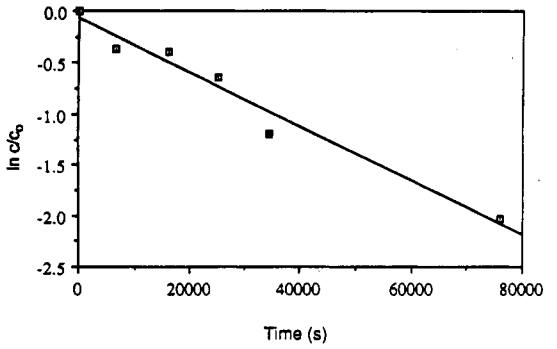

Figure 1. Plot ln (c/c_o) (following ethylene loss) vs time for the hydrosilation of ethylene by 1 in toluene-d_8 at 45 °C, k_{obs} = 2.65 × 10^{-5} s^{-1} (r^2 = 0.968).

Table I. Hydrosilation Rate Data[a]

$[C_2H_4]$ (M)	$[Et_3SiH]$ (M)	k_{obs} (×10^{-5} s^{-1})[b]	k_{2nd} (×10^{-3} M^{-1} s^{-1})[c]
2.31 × 10^{-3}	5.40 × 10^{-2}	2.23	2.62
2.31 × 10^{-3}	7.58 × 10^{-2}	1.61	1.89
2.31 × 10^{-3}	9.67 × 10^{-2}	2.43	2.86
2.31 × 10^{-3}	1.56 × 10^{-1}	2.65	3.12
2.54 × 10^{-3}	1.10 × 10^{-1}	2.38	2.80
2.77 × 10^{-3}	3.91 × 10^{-2}	2.82	3.32
4.62 × 10^{-3}	1.56 × 10^{-1}	1.99	2.34
4.62 × 10^{-3}	2.34 × 10^{-1}	1.94	2.28
9.33 × 10^{-3}	1.56 × 10^{-1}	2.69	3.16
1.29 × 10^{-2}	4.47 × 10^{-1}	4.28[d]	2.23
1.74 × 10^{-2}	1.12 × 10^{-1}	0.566[e]	2.49

[a] Concentration of **1** (or **2b**) = 8.50 × 10^{-3} M unless otherwise stated; solvent = toluene-d_8; T = 45 °C. [b] The error in the value of k_{obs} was calculated to be ±15%. [c] Calculated by dividing k_{obs} by [**2b**]; the error in k_{2nd} was calculated to be ±16%. [d] Concentration of **1** (or **2b**) = 1.92 × 10^{-2} M. [e] Concentration of **1** (or **2b**) = 2.27 × 10^{-3} M.

Scheme IV

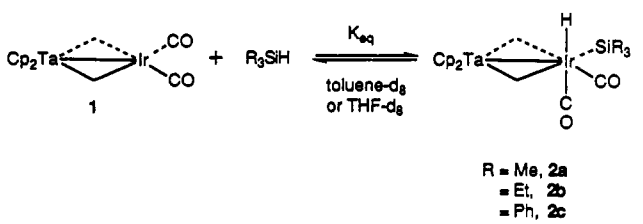

R = Me, **2a**
= Et, **2b**
= Ph, **2c**

order in ethylene. However, subsequent studies revealed that the conclusion was in error: the data collected in Table I and illustrated in Figure 1 demonstrate that the hydrosilation is first-order in the concentration of catalyst and ethylene and independent of [Et_3SiH]. The second-order rate constant for the reaction (the average of the data in Table I) was calculated to be (2.65 ± 0.43) × 10^{-3} M^{-1} s^{-1}. With these measurements in hand, we proceeded to study the stoichiometric steps that might be involved in the overall catalytic cycle.

Synthesis and Characterization of R_3SiH Oxidative Addition Products. Oxidative addition of Me_3SiH to the iridium center of $Cp_2Ta(\mu\text{-}CH_2)_2Ir(CO)_2$ proceeded rapidly at room temperature to establish an equilibrium with the product $Cp_2Ta(\mu\text{-}CH_2)_2Ir(SiMe_3)(H)(CO)_2$ (**2a**) (Scheme IV). Over a broad range of temperatures only one isomer was seen. A single Ir–H resonance (−14.6 ppm), two Cp, and four μ-CH_2 resonances (the two doublets upfield represent one of the CH_2 groups and the two downfield the other as evidenced by the J_{HH} (geminal coupling) values) are present in the ^1H NMR spectra of **2a** (see the Experimental Section). In the ^{13}C NMR spectrum, there are two CO, two CH_2, and two Cp

Scheme V

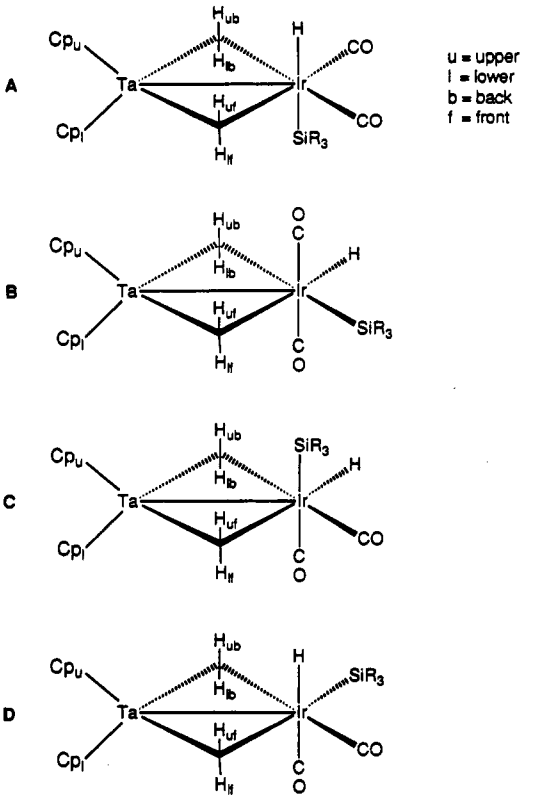

resonances. The solution IR spectrum reveals ν(Ir–H) at 2102 cm^{-1} and two ν(CO) bands at 2024 and 1961 cm^{-1} (ν(Si–H) for free Me_3SiH is also seen). Unfortunately, all attempts to isolate or crystallize **2a** were unsuccessful. The compound was thus characterized only in solution.

Even though there are four possible isomers for the oxidative addition product (Scheme V), only one is formed. By symmetry isomer A (which should exhibit one CH_2 resonance in its ^{13}C NMR spectrum) and isomer B (which should have one Cp resonance in its ^{13}C and ^1H NMR spectra) can be ruled out as possibilities. The two remaining isomers are more difficult to distinguish spectroscopically.

However, on the basis of the following observations, isomer D was chosen as the structure for **2a**. (1) The Cp groups of **2a** have nearly identical chemical shifts in both the ^1H and ^{13}C NMR spectra (Δppm = 0.01 and 0.6, respectively). (2) The two CH_2 groups on the other hand have quite different chemical shifts in both spectra (Δppm = ∼2 and 37, respectively). (3) Consistent with the similar Cp shifts, the hydrogens of each methylene (i.e., within each set of doublets of doublets) do not differ greatly in chemical shift in the ^1H NMR spectra (Δppm = ∼0.1). These observations imply that the back and front quadrants (Scheme V) of the molecule experience strongly differing environments and that the upper and lower quadrants do not. Clearly, the front and back quadrants of C and D are not the same since the trans influences of the ligands (H and CO or $SiMe_3$ and CO) are unequal. However, the upper and lower quadrants of isomer D, with the small H and CO, are sterically similar, whereas in isomer C, the $SiMe_3$ and CO ligands in the upper and lower quadrants vary significantly in size. Consistent with structure D, the J_{HH} values (hydride–CH_2 coupling) for the four CH_2 protons do not follow an obvious pattern. This is not what would be predicted for isomer C, in which

Table II. Equilibrium Data for the System $Me_3SiH + Cp_2Ta(CH_2)_2Ir(CO)_2$ (1) ⇌ $Cp_2Ta(CH_2)_2Ir(H)(SiMe_3)(CO)_2$ (2a) in THF-d_8

T (K)	[Me_3SiH] (M)	[1] (M)	[2a] (M)	K_{eq} (M^{-1})[a]
273	6.09×10^{-3}	1.52×10^{-3}	3.10×10^{-2}	3350
278	5.30×10^{-3}	2.30×10^{-3}	3.02×10^{-2}	2480
283	4.10×10^{-3}	4.53×10^{-3}	2.80×10^{-2}	1510
288	2.56×10^{-3}	6.79×10^{-3}	2.57×10^{-2}	1480
298	3.53×10^{-3}	8.32×10^{-3}	2.42×10^{-2}	824
303	3.96×10^{-3}	9.84×10^{-3}	2.27×10^{-2}	582
313	6.47×10^{-3}	1.05×10^{-2}	2.20×10^{-2}	324

[a] The error limits for K_{eq} were estimated to be ±4% based upon the reproducibility of the values.

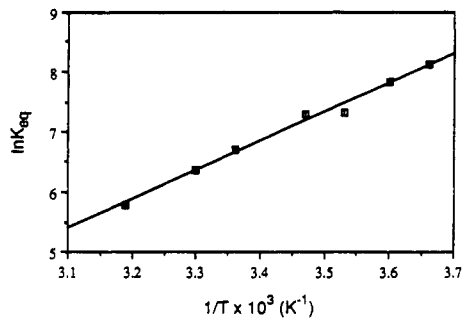

Figure 2. Plot of ln K_{eq} vs T^{-1} for the reaction of 1 and Me_3SiH in THF-d_8. $\Delta H°$ = −9.60 ± 0.45 kcal/mol, $\Delta S°$ = −19.1 ± 1.5 eu (r^2 = 0.989).

the *trans*-hydride methylene coupling should be much greater than the *cis*-hydride methylene coupling.

The equilibrium constant for the reaction of Me_3SiH with $Cp_2Ta(\mu\text{-}CH_2)_2Ir(CO)_2$ in THF-d_8 was measured by ^1H NMR spectrometry over the temperature range 0–40 °C. From these data the thermodynamic parameters for the reaction were calculated: $\Delta H°$ (−9.60 ± 0.45 kcal/mol) and $\Delta S°$ (−19.1 ± 1.5 eu) (Table II and Figure 2).

Triethylsilane also reacts with 1 to establish an equilibrium with its oxidative addition product $Cp_2Ta(\mu\text{-}CH_2)_2Ir(H)(SiEt_3)(CO)_2$ (**2b**) (Scheme IV). Compound **2b** similarly eluded isolation. The ^1H and ^{13}C NMR spectra of **2a** and **2b** are almost identical, and thus D is again predicted to represent the structure of **2b**. Notably, however, the hydride resonance appears slightly upfield relative to that for **2a**, at −14.8 ppm in the ^1H NMR spectrum. The ν(Ir–H) appears at 2095 cm^{-1} and the two ν(CO) stretches at 2025 and 1958 cm^{-1} (also seen is the ν(Si–H) from free Et_3SiH).

The equilibrium constant for the reaction of Et_3SiH with 1 in THF-d_8 was measured by ^1H NMR spectrometry over the temperature range −10 to 40 °C. From a plot of ln K_{eq} vs T^{-1} the enthalpy of reaction $\Delta H°$ = −10.8 ± 0.4 kcal/mol and the entropy of reaction $\Delta S°$ = −24.8 ± 1.4 eu were calculated (Table III). In order to see if solvent polarity had an effect on K_{eq}, the same equilibrium was followed in toluene-d_8 over the temperature range −20 to 70 °C. From the plot of ln K_{eq} vs T^{-1}, the thermodynamic parameters were also calculated: $\Delta H°$ (−11.2 ± 0.7 kcal/mol) and $\Delta S°$ (−25.0 ± 2.5 eu) (Table IV). Within one standard deviation the values for the enthalpy and entropy are the same, and thus any effect of solvent on the equilibrium is minimal. As we reported earlier, a primary equilibrium isotope effect for the reaction of Et_3SiH with 1, $K_{eq}(Et_3SiH)/K_{eq}(Et_3SiD)$ = 0.78, has been calculated from the frequencies of the X–Y [X = Ir, Si; Y = H, D] stretching and bending vibrations observed in the IR

Table III. Equilibrium Data for the System $Et_3SiH + Cp_2Ta(CH_2)_2Ir(CO)_2$ (1) ⇌ $Cp_2Ta(CH_2)_2Ir(H)(SiEt_3)(CO)_2$ (2b) in THF-d_8

T (K)	[Et_3SiH] (M)	[1] (M)	[2b] (M)	K_{eq} (M^{-1})[a]
263	3.50×10^{-3}	1.62×10^{-3}	1.72×10^{-2}	3030
263	3.30×10^{-3}	1.41×10^{-3}	1.74×10^{-2}	3740
273	4.10×10^{-3}	2.15×10^{-3}	1.66×10^{-2}	1780
273	4.20×10^{-3}	2.34×10^{-3}	1.65×10^{-2}	1680
283	5.60×10^{-3}	3.74×10^{-3}	1.51×10^{-2}	721
294	6.70×10^{-3}	4.80×10^{-3}	1.40×10^{-2}	435
303	8.50×10^{-3}	6.55×10^{-3}	1.22×10^{-2}	219
303	8.80×10^{-3}	6.93×10^{-3}	1.19×10^{-2}	207
313	1.01×10^{-2}	8.20×10^{-3}	1.06×10^{-2}	128
313	9.85×10^{-3}	8.00×10^{-3}	1.08×10^{-2}	132

[a] The error limits for K_{eq} were estimated to be ±4% based upon the reproducibility of the values.

Table IV. Equilibrium Data for the System $Et_3SiH + Cp_2Ta(CH_2)_2Ir(CO)_2$ (1) ⇌ $Cp_2Ta(CH_2)_2Ir(H)(SiEt_3)(CO)_2$ (2b) in Toluene-d_8

T (K)	[Et_3SiH] (M)	[1] (M)	[2b] (M)	K_{eq} (M^{-1})[a]
253	1.16×10^{-3}	9.50×10^{-4}	1.13×10^{-2}	10200
273	1.60×10^{-3}	1.40×10^{-3}	1.09×10^{-2}	4870
293	3.55×10^{-3}	3.35×10^{-3}	8.95×10^{-3}	753
313	5.76×10^{-3}	5.56×10^{-3}	6.74×10^{-3}	210
333	8.29×10^{-3}	8.09×10^{-3}	4.21×10^{-3}	62.8
343	9.06×10^{-3}	8.86×10^{-3}	3.44×10^{-3}	42.8

[a] The error limits for K_{eq} were estimated to be ±4% based upon the reproducibility of the values.

Scheme VI

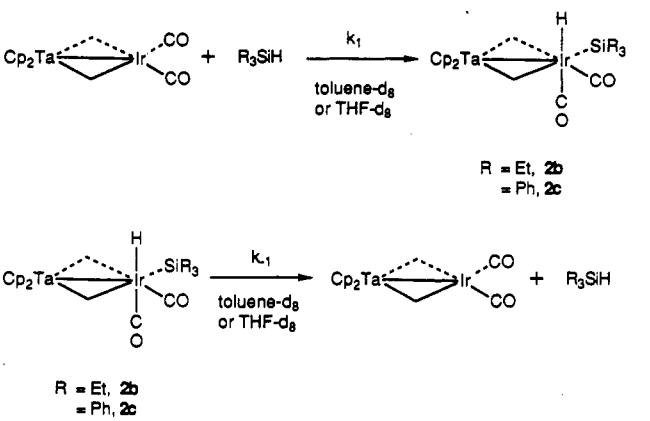

spectra of Et_3SiH, Et_3SiD, 1, and **2b**-d_5 or from literature values of appropriate model compounds.[13]

With the equilibrium data available, we turned to a determination of the rates for the forward and reverse reactions (Scheme VI). As explained in the Experimental Section, the calculation of k_1 and k_{-1} was complicated since an approach to an equilibrium was being measured and thus the rates for both the forward and reverse reaction could only be calculated after obtaining K_{eq} and k_{obs} (the measured rate constant). UV/visible spectroscopy was a useful tool for this purpose because it provided the necessary high accuracy. In general, monitoring was carried out at λ_{max} for each compound followed, except in cases such as the Et_3SiH oxidative addition product where a true maximum was not evident. Each rate was measured three or four times (see Tables V and VI for all measured rate constants). The averaged constants and their stan-

(13) The frequencies used for the isotope effect calculation were the following. Stretching frequencies (cm^{-1}): Si–H, 1978; Si–D, 1494; Ir–H, 2095; Ir–D, 1600. Bending frequencies (cm^{-1}): Si–H, 860; Si–D, 637; Ir–H, 1016; Ir–D, 753. For details of the calculation, see supplementary material supplied with Hostetler, M. J.; Bergman, R. G. *J. Am. Chem. Soc.* **1992**, *114*, 787.

Table V. Rate Data for the Oxidative Addition of Et_3SiH to 1 (k_1) and the Reductive Elimination of Et_3SiH from 2b (k_{-1}) in Toluene

T (K)	k_{obs} (s^{-1})[a]	k_1 (M^{-1} s^{-1})[b]	k_{-1} (s^{-1})[c]
265.2	1.73×10^{-2}	2.04	3.76×10^{-4}
	1.77×10^{-2}	2.09	3.84×10^{-4}
	1.85×10^{-2}	2.18	4.01×10^{-4}
	1.79×10^{-2}	2.11	3.89×10^{-4}
273	3.05×10^{-2}	3.52	1.19×10^{-3}
	3.09×10^{-2}	3.57	1.20×10^{-3}
	3.19×10^{-2}	3.69	1.24×10^{-3}
	3.04×10^{-2}	3.51	1.18×10^{-3}
283	3.87×10^{-2}	7.99	5.56×10^{-3}
	4.31×10^{-2}	8.89	6.20×10^{-3}
	3.43×10^{-2}	7.08	4.94×10^{-3}
	3.56×10^{-2}	7.34	5.12×10^{-3}
293	4.86×10^{-2}	11.3	1.56×10^{-2}
	5.96×10^{-2}	13.9	1.91×10^{-2}
	5.44×10^{-2}	12.7	1.74×10^{-2}
	5.02×10^{-2}	11.7	1.61×10^{-2}
303	9.94×10^{-2}	23.4	6.06×10^{-2}
	9.32×10^{-2}	22.0	5.58×10^{-2}
	10.1×10^{-2}	28.0	6.20×10^{-2}
	9.22×10^{-2}	21.7	5.62×10^{-2}

[a] The error associated with k_{obs} was calculated by the graphing program to be ±1%. [b] The error associated with k_1 was estimated to be ±2%. [c] The error associated with k_{-1} was estimated to be ±6%.

Table VI. Rate Data for the Oxidative Addition of R_3SiH (R = Et, Ph) to 1 (k_1) and the Reductive Elimination of R_3SiH from 2b or 2c (k_{-1})

T (K)	k_{obs} (s^{-1})[a]	k_1 (M^{-1} s^{-1})	k_{-1} (s^{-1})
273[b]	5.80×10^{-3}	2.15	1.31×10^{-3}
	5.86×10^{-3}	2.18	1.32×10^{-3}
	5.92×10^{-3}	2.20	1.34×10^{-3}
	5.76×10^{-3}	2.12	1.29×10^{-3}
283[c]	2.06×10^{-3}	1.28	6.20×10^{-5}
	2.03×10^{-3}	1.26	6.10×10^{-5}
	1.92×10^{-3}	1.20	5.79×10^{-5}
	2.19×10^{-3}	1.36	6.59×10^{-5}

[a] See notes for Table V to explain measurement error. [b] 1 + Et_3SiH ⇌ 2b in THF. [c] 1 + Ph_3SiH ⇌ 2c in THF.

Table VII. Averaged Rate Data for R_3SiH Reactions

reaction	T (°C)	rate
1 + Et_3SiH → 2b in toluene	−7.8	2.10 ± 0.05 M^{-1} s^{-1}
	0	3.57 ± 0.07 M^{-1} s^{-1}
	10	7.82 ± 0.70 M^{-1} s^{-1}
	20	12.4 ± 1.0 M^{-1} s^{-1}
	30	23.8 ± 2.5 M^{-1} s^{-1}
1 + Et_3SiH → 2b in THF	0	2.16 ± 0.03 M^{-1} s^{-1}
1 + Ph_3SiH → 2c in THF	10	1.28 ± 0.06 M^{-1} s^{-1}
2b → 1 + Et_3SiH in toluene	−7.8	(3.88 ± 0.09) × 10^{-4} s^{-1}
	0	(1.20 ± 0.02) × 10^{-3} s^{-1}
	10	(5.46 ± 0.48) × 10^{-3} s^{-1}
	20	(1.70 ± 0.14) × 10^{-2} s^{-1}
	30	(5.86 ± 0.27) × 10^{-2} s^{-1}
2b → 1 + Et_3SiH in THF	0	(1.32 ± 0.02) × 10^{-3} s^{-1}
2c → 1 + Ph_3SiH in THF	10	(6.17 ± 0.28) × 10^{-5} s^{-1}

dard deviations are presented in Table VII. As a double-check, two bands in the UV/vis spectrum were monitored.

The rate of oxidative addition of Et_3SiH to 1 was found to be first-order in [Et_3SiH] and [1]. The oxidative addition of Et_3SiH to 1 in toluene has a second-order rate constant of 3.57 ± 0.07 M^{-1} s^{-1} at 0 °C. The same reaction was also carried out in THF at 0 °C to look for a solvent effect on the rate. The second-order rate constant for the addition of Et_3SiH to 1 was 2.16 ± 0.03 M^{-1} s^{-1}, 40% slower than in toluene. The kinetic isotope effect for this oxidative addition was calculated to be 1.13.[13] Using K_{eq} and k_1, the rate constant for the reductive elimination of Et_3SiH from **2b** at 0 °C (k_{-1}) was calculated to be (1.20 ± 0.02) × 10^{-3} s^{-1} in toluene. The rate for reductive elimination in THF at the same temperature is (1.32 ± 0.02) × 10^{-3} s^{-1}, in this case only 10% faster than in toluene. The kinetic isotope effect for this reductive elimination was found to be 1.45.[13]

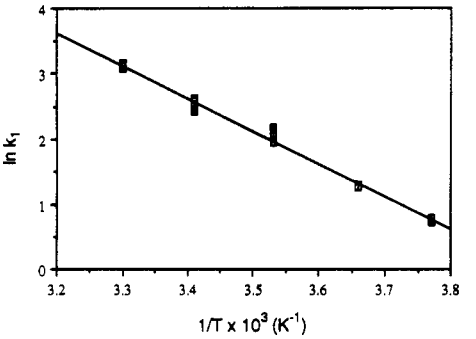

Figure 3. Arrhenius plot for the oxidative addition of Et_3SiH to 1 in toluene. $\Delta H^{\ddagger}$ = 9.4 ± 0.2 kcal/mol, $\Delta S^{\ddagger}$ = −21.1 eu (r^2 = 0.992).

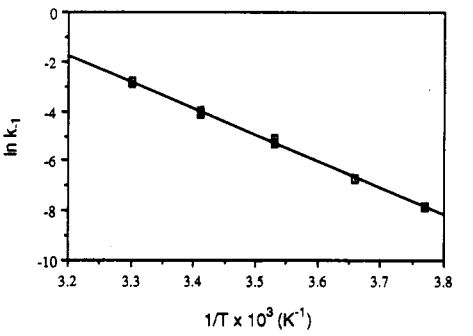

Figure 4. Arrhenius plot for the reductive elimination of Et_3SiH from **2b** in toluene. $\Delta H^{\ddagger}$ = 20.6 ± 0.2 kcal/mol, $\Delta S^{\ddagger}$ = 3.9 eu (r^2 = 0.998).

The activation parameters for the oxidative addition and the reductive elimination of Et_3SiH were determined by measuring the rate for these reactions in toluene over the temperature range −7.8 to 30 °C. A plot of ln k_1 (oxidative addition) vs T^{-1} (Figure 3) gave the enthalpy of activation $\Delta H^{\ddagger}$ = 9.4 ± 0.2 kcal/mol and the entropy of activation $\Delta S^{\ddagger}$ = −21.1 eu. In addition, from the plot of ln k_{-1} vs T^{-1} (Figure 4) the activation parameters for reductive elimination, $\Delta H^{\ddagger}$ = 20.6 ± 0.2 kcal/mol and $\Delta S^{\ddagger}$ = 3.9 eu, were calculated. A complete reaction coordinate is presented in Figure 5.

Addition of Ph_3SiH also establishes an equilibrium in analogy to those described above (Scheme IV). However, in this case, the product $Cp_2Ta(\mu\text{-}CH_2)_2Ir(H)(SiPh_3)(CO)_2$ (**2c**) is insoluble enough in a solution of toluene/pentane to be crystallized at −30 °C. Upon dissolution, the equilibrium is once again established. Because the spectral characteristics of **2c** are very similar to those for **2a** and **2b**, the structure of **2c** is assumed to be isomer D (Scheme V). In the ^1H NMR spectrum the Cp resonance is a sharp singlet, but this must be due to coincidental overlap because two resonances are present in the ^{13}C NMR spectrum. The IR spectrum (KBr) reveals a ν(Ir–H) band at 2123 cm^{-1} (ν(Ir–D) appears at 1600 cm^{-1}) and two ν(CO) stretches at 2031 and 1975 cm^{-1}.

The equilibrium constant for the reaction of Ph_3SiH with $Cp_2Ta(\mu\text{-}CH_2)_2Ir(CO)_2$ in THF-d_8 was measured by ^1H NMR spectrometry over the temperature range 21–65 °C (Table VIII). From these data the thermodynamic parameters for the reaction were calculated: ΔH° (−12.4 ± 0.4 kcal/mol) and ΔS° (−24.0 ± 1.4 eu).

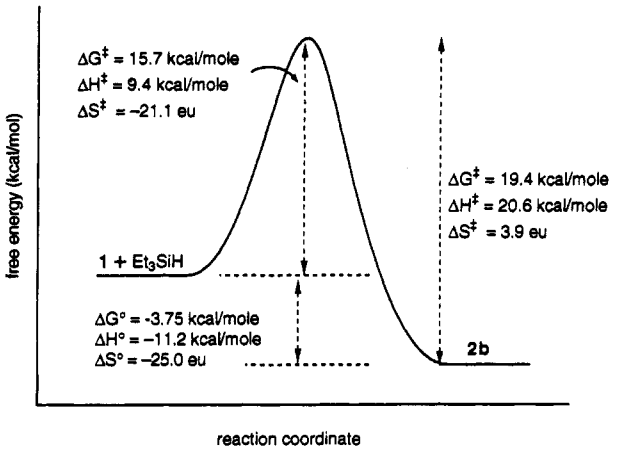

Figure 5. Reaction coordinate diagram for the reaction: $Cp_2Ta(CH_2)_2Ir(CO)_2$ (1) + Et_3SiH ⇌ $Cp_2Ta(\mu\text{-}CH_2)_2Ir(H)(SiEt_3)(CO)_2$ (**2b**). A temperature of 298 K was used for the calculation of the free energy values.

Table VIII. Equilibrium Data for the System Ph_3SiH + $Cp_2Ta(CH_2)_2Ir(CO)_2$ (1) ⇌ $Cp_2Ta(CH_2)_2Ir(H)(SiPh_3)(CO)_2$ (2c) in THF-d_8

T (K)	[Ph_3SiH] (M)	[1] (M)	[2c] (M)	K_{eq} (M^{-1})[a]
294	5.70×10^{-3}	3.13×10^{-4}	1.64×10^{-2}	9190
303	5.90×10^{-3}	5.38×10^{-4}	1.62×10^{-2}	5100
313	6.50×10^{-3}	1.14×10^{-3}	1.56×10^{-2}	2100
318	6.70×10^{-3}	1.30×10^{-3}	1.54×10^{-2}	1770
323	7.00×10^{-3}	1.57×10^{-3}	1.51×10^{-2}	1370
328	7.20×10^{-3}	1.76×10^{-3}	1.49×10^{-2}	1180
333	7.90×10^{-3}	2.48×10^{-3}	1.42×10^{-2}	725
338	8.30×10^{-3}	2.90×10^{-3}	1.38×10^{-2}	573

[a] The error limits for K_{eq} were estimated to be ±4% based upon the reproducibility of the values.

Scheme VII

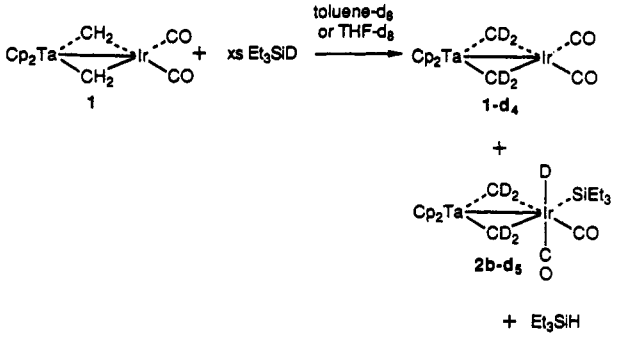

Scheme VIII

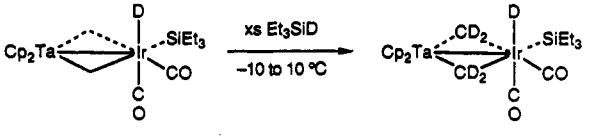

The rate of oxidative addition/reductive elimination of Ph_3SiH in THF at 10 °C was also measured and analyzed as described above (Scheme VI). The second-order rate constant for addition of Ph_3SiH to 1 is 1.28 ± 0.06 M^{-1} s^{-1}, about a factor of 3 slower than the addition of Et_3SiH. The rate of reductive elimination under the same conditions is (6.17 ± 0.28) × 10^{-5} s^{-1}, in this case approximately 100 times slower than the reductive elimination of Et_3SiH.

Exchange Kinetics. Reaction of compound 1 with Et_3SiD produced not only the oxidative addition product, but also resulted in incorporation of deuterium into the bridging methylene positions of 1 and **2b** (Scheme VII). There was an equal percentage of deuterium present in each possible position after the reaction of 1 with 1 equiv of Et_3SiD had reached equilibrium. Addition of an excess of Et_3SiD (>20-fold) resulted in the eventual incorporation of deuterium into all four bridging methylenes.

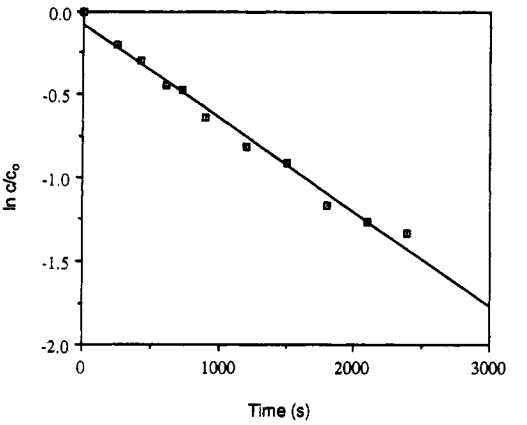

Figure 6. Plot ln (c/c_o) vs time for the incorporation of deuterium into the μ-CH_2 positions of **2b** in toluene-d_8 at 10 °C, k_{obs} = 5.65 × 10^{-4} s^{-1} (r^2 = 0.985).

Table IX. Rate Data for the Exchange of Deuterium into the Methylene Positions of $Cp_2Ta(CH_2)_2Ir(H)(SiEt_3)(CO)_2$ (2b) Using Et_3SiD[a]

T (K)	[**2b**] (M)	[Et_3SiD] (M)	k_{obs} (s^{-1})
263	1.23×10^{-2}	1.77×10^{-1}	7.03×10^{-5}
273	1.23×10^{-2}	8.29×10^{-2}	2.11×10^{-4}
283	1.23×10^{-2}	1.60×10^{-1}	7.28×10^{-4}
283	1.23×10^{-2}	3.68×10^{-1}	5.65×10^{-4}

[a] See the Experimental Section for details of the setup procedure; the estimated error in k_{obs} is ±13%.

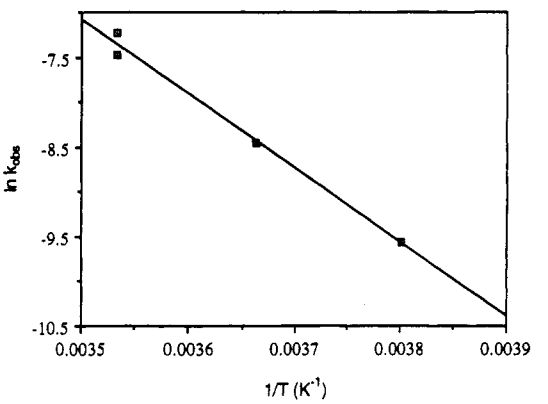

Figure 7. Arrhenius plot for the incorporation of deuterium into the μ-CH_2 groups of **2b** using Et_3SiD, in toluene-d_8. $\Delta H^‡$ = 15.8 ± 1.2 kcal/mol, $\Delta S^‡$ = −17 ± 5 eu (r^2 = 0.990).

The rate of the exchange reaction (Scheme VIII) was measured and found to be first-order in [**2b**] (Figure 6) and zero-order in [Et_3SiD] (compare entries 3 and 4 of Table IX). The first-order rate constant at 10 °C for the incorporation of D into the μ-CH_2 groups in toluene-d_8 is (6.46 ± 0.82) × 10^{-4} s^{-1}. The activation parameters for this reaction, obtained by measuring k_{exc} over the temperature range −10 to 10 °C (at 20 °C, the reaction was too fast to follow by ^1H NMR), were found to be $\Delta H^‡$ = 15.8 ± 1.2 kcal/mol and $\Delta S^‡$ = −17 ± 5 eu (Figure 7; Table IX).

Discussion

Equilibrium Measurements. Addition of R_3SiH to 1 results in the establishment of a measurable equilibrium between the starting materials and the oxidative addition

product **2**. This sort of behavior has been observed in other systems,[14] but there are only a few reports in which a complete determination of the equilibrium constant, thermodynamic parameters $\Delta H°$ and $\Delta S°$, and activation parameters $\Delta H^{\ddagger}$ and $\Delta S^{\ddagger}$ have been made.[15] The reaction enthalpy allows the strength of the Ir–Si bond in this system to be estimated. The bond dissociation energy (BDE) for the Si–H bond in Et_3SiH (90.0 ± 1.0 kcal/mol)[16] and Me_3SiH (90.2 ± 1.1 kcal/mol)[17] have been measured. In addition, the BDE for the Ph_3SiH bond can be estimated as 88 kcal/mol based upon the BDE for the PhH_2Si–H.[18] Based upon the BDE estimated[19] for the average Ir–H bond in $Cp_2Ta(\mu\text{-}CH_2)_2Ir(H)_2(CO)_2$, we can estimate the BDE for the Ir–H bonds to be 50 kcal/mol. These values allow us to estimate an upper limit for the Ir–Si BDE of about 50 kcal/mol. This bond strength does not seem to vary upon changing the groups bound to the silicon. It is interesting to note that the Ir–H and the Ir–Si bond strengths are almost identical. Appearance potentials from mass spectrometric studies have led to the following D(M–Si) values: $(CO)_5Mn$–$SiMe_3$ (61 kcal/mol),[20] $(CO)_5Re$–$SiMe_3$ (72 kcal/mol),[21] $Cp(CO)(PPh_3)Fe$–$SiMe_3$ (51 kcal/mol),[22] $Cp(CO)_2Fe$–$SiMe_3$ (45 kcal/mol).[5,22] Thus, our Ir–Si bond strengths are near the low end of the scale, an especially surprising finding for a third-row metal.

The entropies of reaction for both Et_3SiH and Ph_3SiH are, as expected, nearly equal, but the value for Me_3SiH is noticeably smaller. We currently have no explanation for this effect. The value of the primary equilibrium isotope effect (0.78) indicates that the transition state lies approximately midway along the reaction coordinate.

Kinetic Studies. The measured enthalpies of activation indicate that a substantial amount of bond breaking and/or bond making has occurred in the transition state for both the oxidative addition and reductive elimination reactions.[23] This at first seems inconsistent with the small kinetic isotope effects (KIEs) that have been measured for the k_1 (1.13) and k_{-1} (1.45) steps.[13] Even smaller KIE values were measured for the oxidative addition of Ph_3SiH (1.05) to $CpMn(CO)_2$ and for its reductive elimination from $CpMn(CO)_2(H)(SiPh_3)$ (0.97).[24] Both a nonlinear transition state (η^2-bound Et_3SiH) and a preequilibrium involving a σ-complex (η^1-bound Et_3SiH) provide possible explanations for these data. The moderately sized $\Delta S^{\ddagger}$ for the oxidative addition and the small $\Delta S^{\ddagger}$ for the reductive elimination observed in our system support both proposals, and thus we cannot distinguish between the two at this time.

A broad range of activation parameters has been reported for other silane oxidative addition reactions. For the addition of $(EtO)_nMe_{(3-n)}SiH$ to $Ir(diphos)_2{}^+BPh_4{}^-$ values fall in the range 5.6–5.8 kcal/mol for $\Delta H^{\ddagger}$ and −46.5 to −48.2 cal deg^{-1} mol^{-1} for $\Delta S^{\ddagger}$;[15] for the addition of Et_3SiH to $(\eta^n\text{-}C_nR_n)M(CO)_2$ the values for $\Delta H^{\ddagger}$ are between 7 and 10 kcal/mol and for $\Delta S^{\ddagger}$, −7 to +11.2 cal deg^{-1} mol^{-1}.[25] Thus, our $\Delta H^{\ddagger}$ falls near the upper end of the scale, whereas our $\Delta S^{\ddagger}$ is intermediate in magnitude. Similarly, for reductive elimination the range for $\Delta H^{\ddagger}$ is 19–29 kcal/mol and for $\Delta S^{\ddagger}$, 0–16 cal deg^{-1} mol^{-1}.[15,24] Thus our $\Delta H^{\ddagger}$ and $\Delta S^{\ddagger}$ are both near the lower end of the spectrum.

Scheme IX

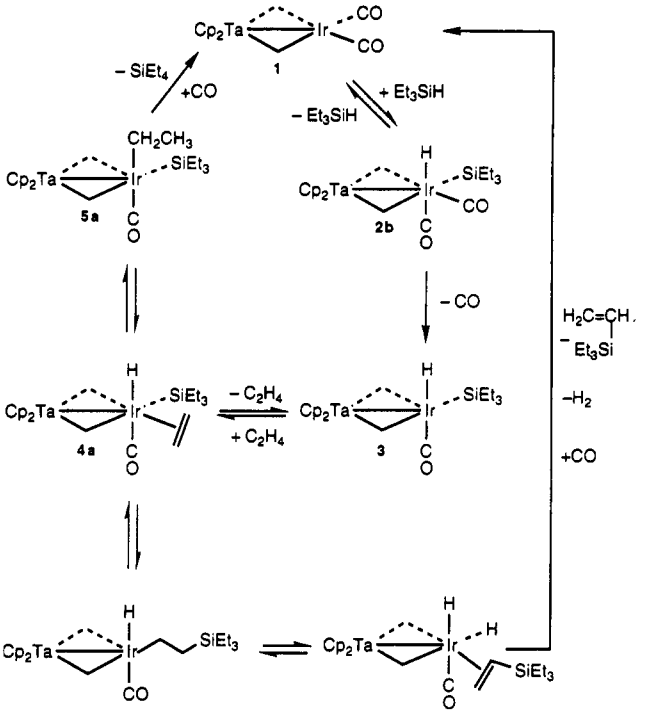

Triphenylsilane adds more slowly than Et_3SiH to **1**, likely due to its greater steric requirements. However, this is not reflected in the rate of reductive elimination, which actually is much slower than that observed for Et_3SiH. This may mean that the Ir–$SiPh_3$ bond is slightly stronger than the Ir–$SiEt_3$ bond, perhaps due to its ability to withdraw electron density from the already electron-rich iridium.[5,15] Similar behavior is seen when comparing the K_{eq} values for the reaction of **1** with PEt_3 vs PPh_3.[26]

Proposed Mechanisms for Deuterium Exchange and Ethylene Hydrosilation. The proposed mechanism for the hydrosilation of ethylene catalyzed by **1** is presented in Scheme IX, and for exchange of deuterium into the bridging methylene positions of the catalyst in Scheme X. As can be seen, we believe that the pathways involving deuterium exchange and hydrosilation diverge after oxidative addition of Et_3SiH, which is proposed to be the first step of the reaction. Because more than 2 equiv of silane essentially drove the equilibrium completely toward the oxidative addition complex **2**, the sole metal species observed during both kinetic studies was **2b**. Therefore, in both cases, zero-order dependence on the concentration of the silane was observed.

We do not yet understand the mechanism of formation of the (minor) vinylsilane product. Alkenes have been reported to insert into the M–Si bond in several other

(14) Collman, J. P.; Hegedus, L. S.; Norton, J. R.; Finke, R. G. *Principles and Applications of Organotransition Metal Chemistry*; University Science Books: Mill Valley, 1987; p 565.
(15) Harrod, J. F.; Smith, C. A. *J. Am. Chem. Soc.* **1970**, *92*, 2699.
(16) Kanabus-Kaminska, J. M.; Hawari, J. A.; Griller, D.; Chatgilialoglu, C. *J. Am. Chem. Soc.* **1987**, *109*, 5267.
(17) Walsh, R. *Acc. Chem. Res.* **1981**, *14*, 246.
(18) Walsh, R. In *The Chemistry of Organic Silicon Compounds*; Patai, S., Rappoport, Z., Eds.; John Wiley & Sons Ltd: New York, 1989; p 371.
(19) Hostetler, M. J.; Butts, M. D.; Bergman, R. G., submitted for publication.
(20) Burnham, R. A.; Stobart, S. R. *J. Chem. Soc., Dalton Trans.* **1973**, 1269.
(21) Burnham, R. A.; Stobart, S. R. *J. Chem. Soc., Dalton Trans.* **1977**, 1489.
(22) Spalding, T. R. *J. Organomet. Chem.* **1978**, *149*, 371.
(23) Lowry, T. H.; Richardson, K. S. *Mechanism and Theory in Organic Chemistry*, 3rd ed.; Harper and Row: New York, 1987; pp 212–214.
(24) Hart-Davis, A. J.; Graham, W. A. G. *J. Am. Chem. Soc.* **1971**, *94*, 4388.
(25) Hill, R. H.; Wrighton, M. S. *Organometallics* **1987**, *6*, 632.
(26) Hostetler, M. J.; Butts, M. D.; Bergman, R. G. *Inorg. Chim. Acta* **1992**, *198–200*, 377.

Scheme X

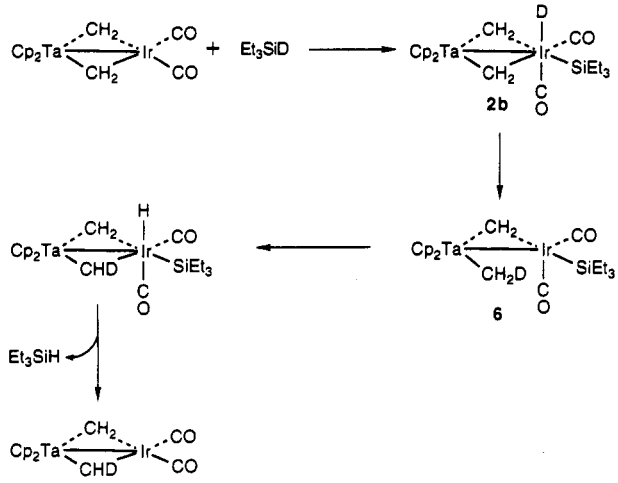

Table X. Hydrosilation Product Ratio Data

[1] (mM)	[Et_3SiH] (mM)	[C_2H_4] (mM)	yield of $Et_3Si(CHCH_2)$ (%)[a]
8.50	139.5	5.26	16.2
	37.5	24.5	29.8
	15.0[b]	14.4	23.3
	39.6	120.9	14.9
	18.6[b]	71.5	12.7
	25.2[b]	150	9.8
8.45	35.5	24.6	14.8[c]
	41.6	142.9	13.7[c]
8.52	34.9	119.3	19.0[d]
9.54	39.6	132.7	16.2[e]

[a] Yields were determined by ^1H NMR spectroscopy and gas chromatography. [b] In these reactions the silane was added by vacuum transfer rather than by syringe. [c] These reactions contain excess CO (see the Experimental Section). [d] 1,3,5-Trimethoxybenzene was used as internal standard. [e] No internal standard was used. The product ratio was determined by integrating against the Cp resonances of **1** in the ^1H NMR spectrum.

systems, including other Ir complexes.[5-7,12,27-30] As can be seen from Table X, in our system the yield of vinylsilane varies between 10 and 30% from run to run. As noted earlier, this does not appear to be caused by an analytical problem: in any given run the vinylsilane/tetraethylsilane ratio does not depend on the extent of conversion, and ratios measured by NMR and gas chromatography are in good agreement. We do not understand this behavior. However, the yield of vinylsilane is always below 30%, no matter what [R_3SiH] is used. This behavior differs markedly from that observed in some earlier studies,[6,12] where the use of high reactant silane concentrations caused vinylsilane to become the major product. If, in the interests of parsimony, we assume that the tetraethylsilane and vinyltriethylsilane are produced in the same cycle,[31] the simplest way to account for the formation of vinylsilane in our system is to propose that insertion of ethylene into the Ir–Si bond in **4a** competes to a minor extent with the predominant alkene/M–H insertion pathway illustrated in Scheme IX.[32] The minor insertion product formed in this way can then undergo β-elimination/reductive elimination to give vinylsilane and H_2. However, at present we cannot rule out the alternative possibility that the erratic yields of vinylsilane are not produced by **1** but by a soluble catalytically active impurity that is present in varying amounts from run to run.

The mechanism of deuterium exchange (Scheme X) is similar to that proposed for exchange involving D_2.[19] That is, reductive elimination of a methylene deuteride occurs from **2b** to form intermediate **6**. This complex can be considered as $Cp_2Ta(CH_2)(CH_3)$ η^2-bound to $Ir(SiR_3)(CO)_2$. Unfortunately, a crossover experiment involving addition of $Cp_2Ta(CD_2)(CD_3)$ to the reaction mixture could not be performed since $Cp_2Ta(CH_2)(CH_3)$ reacts with silanes.[33] However, the products known to be formed in this reaction[33] were not observed under the hydrosilation conditions. Therefore, it appears that the dinuclear Ta/Ir system retains its integrity throughout the reaction. The exchange reaction then proceeds by oxidative addition of the Ta–CH_2D group of **6** across the iridium to reform **2b**, and reductive elimination of Et_3SiH completes the cycle. Under an excess of Et_3SiD, all four of the μ-CH_2 positions can become deuterated.

It is likely that alkene can bind to the coordinatively unsaturated iridium center of **6** (Scheme X). However, we believe that the pathway for hydrosilation does not proceed via this route based on the following pieces of evidence: (1) CO dissociates at room temperature from the six-coordinate species $Cp_2Ta(\mu\text{-}CH_2)_2Ir(Me)(I)(CO)_2$ (**8**)[34] and likely can also dissociate from **2b** to form **3**. This is probably not the rate-determining step in hydrosilation since CO dissociation from **8** occurs at room temperature whereas hydrosilation is only observed at 45 °C. Since binding of ethylene to **3** to form **4a** (Scheme IX) occurs before the rate-determining step, its concentration appears in the rate law. (2) Addition of an overpressure of CO to a hydrosilation reaction solution (run with a significant excess of silane, so that the sole observable metal complex was **2b**) severely inhibits the rate of Et_4Si formation, directly indicating that CO dissociation is involved in the mechanism.

Isomerization of the substituted alkenes likely occurs after CO dissociation: first by binding alkene to **3** and then inserting into the Ir–H bond, followed by β-elimination (Scheme XI). Reductive elimination of R_4Si from these (alkyl)(silyl)metal complexes may be energetically unfavored due to poor orbital overlap. Consistent with this, the least sterically congested alkene is the only one that is hydrosilated.

Stimulated by Perutz's suggestion that two molecules of silane might be involved in a hydrosilation process,[6] we considered the possibility of a mechanism involving oxidative addition of 2 mol of silane occurring in our system (Scheme XII). It is possible that reductive elimination of a methylene bridge (similar to the critical step suggested for the mechanism of H_2/D_2 exchange and alkene hydrogenation) in intermediate **4a** could return the iridium center to the formal +1 oxidation state, allowing a second

(27) Randolph, C. L.; Wrighton, M. S. *J. Am. Chem. Soc.* **1986**, *108*, 3366.
(28) Reichel, C. L.; Wrighton, M. S. *Inorg. Chem.* **1980**, *19*, 3858.
(29) Schroeder, M. A.; Wrighton, M. S. *J. Organomet. Chem.* **1977**, *128*, 345.
(30) Wakatsuki, Y.; Yamazaki, H.; Nakano, M.; Yamamoto, Y. *J. Chem. Soc., Chem. Commun.* **1991**, 703.
(31) Supporting this assumption is the fact that hydrosilation reactions run under CO gave yields of vinylsilane comparable to those observed in the absence of CO.
(32) This explanation for the production of vinylsilane requires that intermediate **4a** is capable of undergoing insertion of ethylene into the M–Si bond, but that for some reason this process is slower in the complex formed by coordination of ethylene to **6**. Perhaps this is a consequence of the different formal oxidation states of the two intermediates.
(33) Berry, D. H.; Koloski, T. S.; Carroll, P. J. *Organometallics* **1990**, *9*, 2952.
(34) Hostetler, M. J. Ph.D. Thesis, University of California, Berkeley, 1992.

Scheme XI

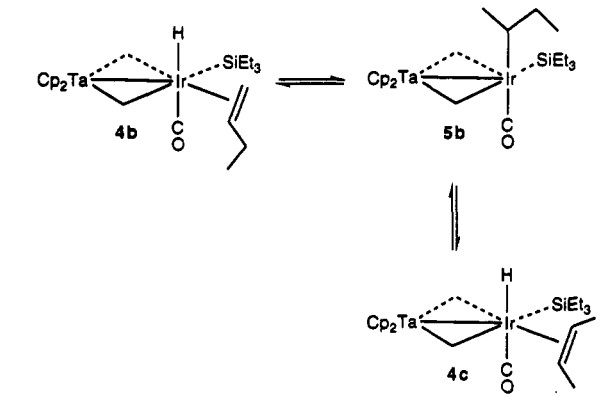

Scheme XII

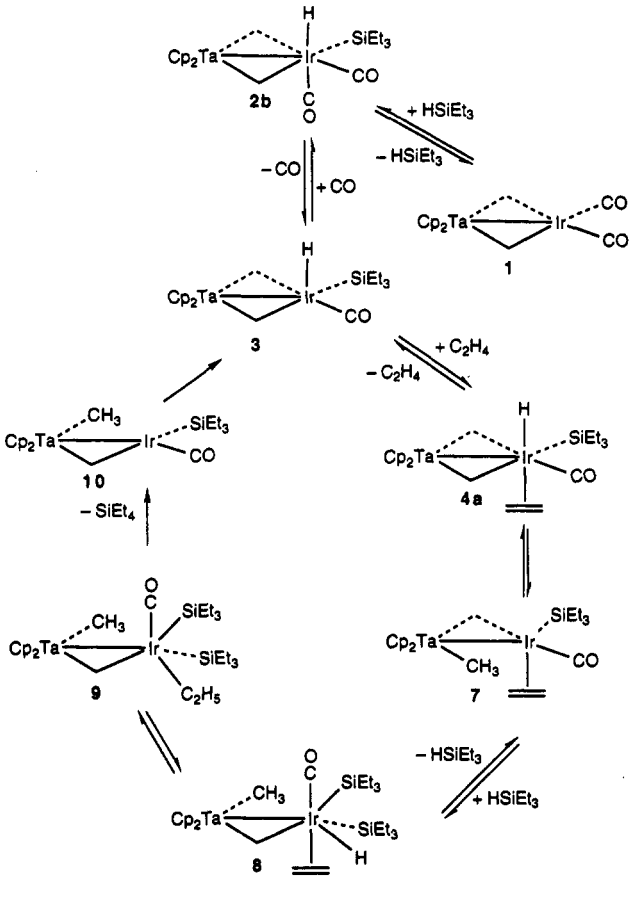

silane to add to the late metal center. As long as ethylene binding to **3** or conversion of **4a** to **7** is rate determining, this mechanism is kinetically indistinguishable from that proposed in Scheme IX. However, compound **1** isomerizes but does not hydrosilate 1-butene. If the Perutz mechanism were workable for the isomerization reaction, isomerization would have a dependence on [$HSiEt_3$]. When two parallel 1-butene isomerizations were set up with differing silane concentrations (1.24×10^{-2} and 4.14×10^{-2} M), the rates were qualitatively identical. Thus, the mechanism outlined in Scheme XII cannot be operative in our system.

Summary and Conclusions. The reversibility of silane oxidative addition to $Cp_2Ta(\mu\text{-}CH_2)_2Ir(CO)_2$ (**1**) has allowed us to carry out a detailed study of the kinetics and thermodynamics of this process, which we offer as the main contribution of this paper. It seems clear that these steps initiate the conversion of ethylene to tetraethylsilane catalyzed by **1**, as well as the exchange of deuterium from Et_3SiD into the bridging methylene groups of the catalyst. Addition of mercury does not affect catalyst activity, and so this reaction appears to be truly homogeneous. Because the addition of CO inhibits the rate of hydrosilation in the presence of excess Et_3SiH, where oxidative addition product **2b** is the resting state of the catalyst, we believe that deuterium exchange and hydrosilation diverge at this point. At present the mechanisms illustrated in Schemes IX and X are the simplest that we can propose for these overall processes. However, there are a number of aspects of the reaction that remain to be elucidated, the most perplexing of which is the peculiar variation of the yield of vinylsilane. It appears that hydrosilation catalyzed by **1**, like that mediated by several more well-established catalysts, will require further study before a full understanding of its mechanism is achieved.

Table XI. Reaction Parameters for Setting Up the Thermodynamic Studies[a]

reaction	solvent	vol of solv (mL)	[1] (M)	silane (μmol)
1 + Et_3SiH	toluene-d_8	0.55	1.23×10^{-2}	6.81
1 + Et_3SiH	THF-d_8	0.48	1.88×10^{-2}	9.92
1 + Me_3SiH	THF-d_8	0.44	3.25×10^{-2}	14.3
1 + Ph_3SiH	THF-d_8	0.52	1.67×10^{-2}	11.5

[a] See the Experimental Section for a description of the setup procedure.

Experimental Section

General. Unless otherwise noted, all reactions and manipulations were performed in dry glassware under a nitrogen atmosphere in a Vacuum Atmospheres 553-2 drybox equipped with an M6-40-1H Dri-train or using standard Schlenk techniques.

Benzene, toluene, and THF were distilled from sodium/benzophenone. Pentane was distilled from lithium aluminum hydride. Triethylsilane and triisopropylsilane were distilled from activated 4-Å molecular sieves. Triethylsilane-d_1 was synthesized from triethylsilyl chloride and $LiAlD_4$. The synthesis and characterization of $Cp_2Ta(\mu\text{-}CH_2)_2Ir(CO)_2$ was presented in a previous paper.[26] Unless otherwise noted, all other reagents were used as received from commercial suppliers.

Generation of $Cp_2Ta(\mu\text{-}CH_2)_2Ir(CO)_2(H)(SiMe_3)$ (2a) in Solution. A solution of 22 mg of **1** (37 μmol) in 0.45 mL of C_6D_6 was prepared in the drybox and added to a Wilmad PS-505 NMR tube. This was connected to a Kontes vacuum adaptor via a Cajon joint.[35] The tube was brought out of the drybox, connected to a vacuum line, frozen and degassed. While keeping this solution at 77 K, 51 μmol of Me_3SiH was transferred into the tube. The NMR tube was then sealed and the solution thawed. The color of the solution immediately changed from yellow to nearly colorless. Because **2a** is in equilibrium with free Me_3SiH and **1**, an excess of Me_3SiH was added to drive the reaction to >95% completion. All spectra were taken on this solution (resonances due to the excess Me_3SiH were determined from spectra of the free material in C_6D_6): ^1H NMR (C_6D_6) δ 6.22 (dd, J = 8.7, 2.4 Hz, 1 H), 6.16 (dd, J = 8.7, 1.2 Hz, 1 H), 4.49 (s, 5 H), 4.48 (s, 5 H), 4.21 (dd, J = 9.3, 2.4 Hz, 1 H), 4.06 (dd, J = 8.7, 1.2 Hz, 1 H), 1.04 (s, 9 H), −14.6 (m, 1 H); ^{13}C NMR (C_6D_6) δ 179.1 (s), 175.7 (s), 107.0 (s), 100.4 (s), 99.8 (s), 69.7 (s), 10.0 (s); IR (C_6D_6) 2102, 2024, 1961 cm^{-1}. All attempts to isolate this complex returned starting material **1**.

Generation of $Cp_2Ta(\mu\text{-}CH_2)_2Ir(CO)_2(H)(SiEt_3)$ (2b) in Solution. A solution of 21 mg of **1** (36 μmol) in 0.45 mL of C_6D_6

(35) Bergman, R. G.; Buchanan, J. M.; McGhee, W. D.; Periana, R. A.; Seidler, P. F.; Trost, M. K.; Wenzel, T. T. In *Experimental Organometallic Chemistry: A Practicum in Synthesis and Characterization*; ACS Symposium Series 357; Wayda, A. L., Darensbourg, M. Y., Eds.; American Chemical Society: Washington, DC, 1987; p 227.

Table XII. Experimental Parameters Used for Oxidative Addition Kinetic Studies[a]

reaction (solvent)	T (°C)	[1] (M)	[R_3SiX] (M)[b]	λ (nm)[c]	reaction time (s)[d]	Δ points (s)[e]
1 + Et_3SiH (toluene)	−7.8	2.45×10^{-4}	8.31×10^{-3}	354, 404	4 × 300	15
1 + Et_3SiH (toluene)	0	2.38×10^{-4}	8.31×10^{-3}	404	2 × 180, 2 × 200	10, 10
1 + Et_3SiH (toluene)	10	2.34×10^{-4}	4.16×10^{-3}	352, 404	4 × 120	6
1 + Et_3SiH (toluene)	20	2.34×10^{-4}	2.91×10^{-3}	352, 404	4 × 100	5
1 + Et_3SiH (toluene)	30	1.81×10^{-4}	1.66×10^{-3}	351, 404	4 × 60	3
1 + Et_3SiH (THF)	0	1.08×10^{-4}	2.09×10^{-3}	282, 402	5 × 720	40
1 + Et_3SiD (toluene)	0	2.38×10^{-4}	8.31×10^{-3}	404	2 × 180, 2 × 200	10, 10
1 + Ph_3SiH (THF)	10	1.00×10^{-4}	1.56×10^{-3}	280, 402	2 × 1190, 2 × 1440	70, 80

[a] See the Experimental Section for a description of the setup procedure. [b] Concentration of the substrate which was oxidatively added to the iridium complex. [c] Wavelength(s) at which the reaction was monitored. [d] Length of time over which the reaction was monitored. [e] Time between spectra during the kinetics run.

was added to a Wilmad PS-505 NMR tube. The reaction was treated as for **2a**, except Et_3SiH was added (52 μmol). Under these conditions the equilibrium was shifted quantitatively to **2b**: ^1H NMR (toluene-d_8) δ 6.22 (s, 2 H), 4.54 (s, 5 H), 4.52 (s, 5 H), 4.15 (dd, J = 9.3, 1.2 Hz, 1 H), 3.96 (dd, J = 9.3, 5.7 Hz, 1 H), 1.28 (m, 15 H), −14.8 (m); ^{13}C NMR (C_6D_6) δ 179.6 (s), 178.2 (s), 107.7 (s), 100.4 (s), 100.0 (s), 67.2 (s), 12.3 (s), 9.92 (s); IR (THF-d_8) 2095, 2025, 1958 cm^{-1}. All attempts to isolate this complex returned starting material 1.

$Cp_2Ta(\mu\text{-}CH_2)_2Ir(CO)_2(H)(SiPh_3)$ (2c). (a) For Isolation. To a solution of 50 mg of 1 (85 μmol) in 5 mL of benzene was added 34.4 mg of Ph_3SiH (128 μmol). The mixture was stirred until the yellow solution became colorless. This solution was transferred to a scintillation vial and layered with 10 mL of pentane. White crystalline blocks (46 mg; 55%), which formed upon cooling this solution to −30 °C, were collected on a glass frit by suction filtration.

(b) For Spectrometric Characterization. A solution of 15 mg of 1 (26 μmol) and 9 mg of Ph_3SiH (35 μmol) in 0.5 mL of THF was placed in a Wilmad PS-505 NMR tube. The resonances due to free Ph_3SiH were assigned based on spectra of the pure compound: ^1H NMR (C_6D_6) δ 8.02 (m, 6 H), 7.37 (m, 9 H), 6.22 (d, J = 8.7 Hz, 1 H), 6.13 (dd, J = 8.7, 1.8 Hz, 1 H), 4.44 (s, 10 H), 4.08 (d, J = 9.6, 1 H), 4.07 (d, J = 9.6, 1 H), −14.3 (br s, 1 H); ^{13}C NMR (C_6D_6) δ 178.1 (s), 174.8 (s), 145.4 (s), 136.8 (s), 127.8 (s), 127.5 (s), 106.6 (s), 100.3 (s), 100.2 (s), 74.8 (s); IR (KBr pellet) 2123, 2031, 1975, 1427, 1089, 836, 702, 513 cm^{-1}. Anal. Calcd for $C_{32}H_{30}IrO_2SiTa$: C, 45.33; H, 3.56. Found: C, 45.67; H. 3.64.

Thermodynamic Measurements and Calculations: General. A weighed amount of 1 was dissolved in approximately 0.45 mL of the NMR solvent and the resulting solution added to a Wilmad PS-505 NMR tube. Ph_3SiH (a weighed amount) was also added at this time. The tube was then set up as described above. Et_3SiH or Me_3SiH was added to the NMR tube by vacuum transfer, waiting at least 10 min for the transfer because the silanes tend to condense slowly. All tubes were flame-sealed, thawed, and then allowed to stand at room temperature for 3 h in order to reach equilibrium. The exact solution volume (and thus, the reagent concentrations) was calculated by measuring the height of the meniscus in the tube and then calibrating this measurement with known amounts of solvent in four Wilmad PS-505 NMR tubes. This showed that 1.00 mL reproducibly gave a solvent height of 74.5 ± 0.2 mm. The reactions were monitored using a 300-MHz NMR spectrometer with a calibrated thermocouple placed in the probe. The samples were equilibrated at each temperature for 10 min before taking the spectrum. Spectra were then sequentially obtained as the probe was heated to the maximum temperature and then again as the probe was cooled to the minimum temperature, and thus two points were obtained for each temperature (the K_{eq} values agreed to within 5%). Concentrations of the molecules were measured against ferrocene as the internal standard, and K_{eq} was calculated using standard equations. Plots of ln K_{eq} vs $1/T$ were made using the Igor graphing program[36] and the reported standard deviations obtained from the best fit of the line to the points. See Table XI for the experimental parameters used for each individual run.

Kinetics: UV/Vis, General. Standard solutions were prepared in the drybox in volumetric flasks and stored in the drybox freezer at −30 °C. Individual runs were prepared in the drybox by transferring aliquots of standard solutions using a graduated pipet into a quartz cuvette fused to a Kontes vacuum adapter equipped with a stir bar, a 14/20 rubber septum (for the ground glass joint) and a 24/40 rubber septum (to fit over the top of the screw joint, the Kontes teflon stopcock was not used). The sample was taken out of the drybox and placed into a Hewlett-Packard temperature-controlled cell holder (equipped with a magnetic stirrer and a nitrogen gas inlet to prevent water condensation). UV/vis spectra were taken once/min until the peak intensities were stable, at which point the solution was assumed to be thermally equilibrated. The reactant (kept in a vial under N_2) was added via a calibrated 10-μL syringe, and the preprogrammed kinetics run was initiated. Spectra were recorded, in general, three times during every half-life for 7 half-lives. If possible, reactions were followed at one wavelength in the visible region and one wavelength in the UV region. See Table XII for the experimental parameters used for each individual run.

Plots of A (related to c/c_0 by Beer's law) or ln $(A_\infty/(A - A_\infty))$ (for decreasing absorbances) or ln $(A_\infty/(A_\infty - A))$ (for increasing absorbances) (A = measured absorbance intensity, A_∞ = infinity value of absorbance intensity, c = concentration at time t, c_0 = initial concentration) vs time were plotted using the Igor graphing program.[36,37] Least-squares fits of the data were also performed by the software in the program to give as the slope the pseudo-first-order rate constant for the reactions. Second-order rate constants were calculated by standard kinetic equations.[38]

Because the silane oxidative addition reactions did not go to completion, but approached an equilibrium, the slope (k_{obs}) of the $ln\ (A_\infty/(A - A_\infty))$ vs t plots for the reaction was equal to $k_1[R_3SiX] + k_{-1}$. From the measured values of K_{eq} and k_{obs}, the second-order rate constant for oxidative addition (k_1) and the first-order rate constant for reductive elimination (k_{-1}) were calculated.

Activation parameters for the oxidative addition of Et_3SiH to 1 and the reductive elimination of Et_3SiH from **2b** were obtained by plotting ln k_1 or ln k_{-1} versus $1/T$ to give a typical Arrhenius plot. From the values of the slope and y-intercept the enthalpy and entropy of activation were calculated using standard equations.

Determination of the Rate and Kinetic Parameters for Deuterium Exchange by Et_3SiD. Approximately 0.4 mL of a standard solution of 1 (1.23×10^{-2} M) and Cp_2Fe (internal standard, 5.86×10^{-3} M) in toluene-d_8 were added to a Wilmad PS-505 NMR tube. After the solution was frozen at 77 K and degassed once, a measured quantity of Et_3SiD (Table IX) was vacuum-transferred into the solution. The tube was flame-sealed and kept frozen until directly before the kinetic run. Because

(36) The Igor graphing and data analysis software are distributed by WaveMetrics of Lake Oswego, OR.

(37) The Igor graphing program was modified by Dr. Kevin Kyle to calculate the infinity point and rate constant for a first-order reaction.

(38) Benson, S. W. *The Foundations of Chemical Kinetics*; McGraw-Hill: New York, 1960.

of the complexity of the ^1H NMR spectrum, the reaction was monitored by following the appearance of the Si–H resonance. The data were worked up as described above.

Hydrosilation Reactions: Determination of the Rate Law. Approximately 0.5 mL of a standard solution of 1 and 1,3,5-trimethoxybenzene (internal standard) in toluene-d_8 was added to a Wilmad PS-505 NMR tube. After the solution was frozen at 77 K and degassed once, measured quantities of Et_3SiH and C_2H_4 were vacuum transferred into the solution (refer to Table I for individual [1], [Et_3SiH], and [C_2H_4]). The tube was flame-sealed and kept frozen until directly before the kinetic run. The reaction was monitored by following the disappearance of the ethylene resonance in the ^1H NMR spectrum (formation of Et_4Si could not be monitored due to overlap of the Et_3SiH and Et_4Si alkyl resonances). The CO inhibition experiment was performed by adding ~1200 Torr of CO to a typical hydrosilation solution; less than 5% reaction was observed by ^1H NMR spectrometry after 24 h at 45 °C. The data were worked up as described above.

Hydrosilation Reactions: Determination of Vinylsilane Yield. Approximately 0.5 mL of a standard toluene-d_8 solution of 1 (8.50 mM) and ferrocene (internal standard, 7.92 mM) was measured out. A determined quantity of Et_3SiH was added by syringe to the solution which was then transferred to an NMR tube. The solution was frozen at 77 K and degassed once. A measured amount of C_2H_4 was added to the tube by vacuum transfer (see Table X for individual [1], [Et_3SiH], and [C_2H_4]). The tube was then flame-sealed. The reactions were run in a constant temperature bath maintained at 45 °C and were monitored periodically by ^1H NMR spectroscopy. The yields of vinylsilane were taken to be the average of those yields determined by ^1H NMR spectroscopy (integrating the vinyl resonances against the internal standard after the reaction was concluded, i.e., after all of the starting material in limiting concentration had been consumed) and gas chromatography. The hydrosilation reactions run in the presence of excess CO were set up in an analogous manner except that approximately 5 equiv of CO (47 Torr, 2.25 mL, 2.2×10^{-5} mol) were added to the NMR tube immediately following the condensation of ethylene.

Acknowledgment. We would like to thank Johnson Matthey Aesar/Alfa for a generous loan of iridium and the National Science Foundation (Grant No. CHE-9113261) for financial support of this work.

OM920144P